1-

TRANSIENT PERFORMANCE OF A 5-PH BRUSHLESS DC GENERATOR

2-

3- W.R. Gerges*, J.G. Kettleborough** and I.R. Smith***

4- ABSTRACT

The paper studies the transient performance of a 28 V, 14 KW brushless 5-phase DC genertor, with its associated automatic voltage regulator (AVR). The study describes the performance of the generator when subjected to sudden increase and sudden decrease in load as well as the case when the generator is connected to a dynamic load which may regenerate power into the generator. A mathematical model is developed for the system to enable these studies to be carried out. Modelling of the generator/rectifier and exciter/rectifier arrangements is achieved using tensor methods to define the changing conduction pattern of the diodes in the rectifier bridges owing to the local ocnditions and the changing magnitudes of the armature voltages. The AVR is modelled in terms of the actual configuration, rather than by the more familiar transfer function approach, and the resulting differential equations are integrated together with those for the generator and the exciter. Experimental results are presented in excellent agreement with those from the computer predictions, thereby validating the model and illustrating its use as a valuable tool for engineers involved in the design of control systems containing electrical machines.

* Lecturer, The Air Defence Academy, Alexandria, Egypt.

5- ** S. Lecturer, University of Technology, Loughborough, England.

*** Head of Electricl Department, University of technology, Loughborough, England.

LIST OF PRINCIPAL SYMBOLS

In the list below, suffixes b and m refer respectively to the branch and mesh reference frames.

$E_b, E_m; V_b, V_m$ = voltage source and voltage vectors respectively.

I^b, I^m = current vectors

$R_b, R_m ; L_b, L_m$ = resistance and inductance matrix respectively

G_b, G_m = rate-of-change of inductance matrices.

$C^b_{.m} ; c^{.m}_b$ = mesh/branch current and branch/mesh voltage transromation matrices respectively

$p = \frac{d}{dt}$

I_{Gn} = generator output current

I_B = battery/capacitor mesh current

I_{bt} = battery branch current

E_{bt} = battery voltage

E_L = voltage source representing dynamic load

I_L = load current

R_L, L_L = load resistance and inductance

R_{bt}, L_{bt} = battery resistance and inductance

R_{tl}, L_{tl} = cable resistance and inductance

V_{bt} = battery branch voltage

V_c = voltage across capacitor C.

1- INTRODUCTION :

Mobil and fighting vehicles often require a high-performance electrical power supply, which is frequently provided by a regulated and brushless DC generator. Fig. 1. shows the arrangement of typical unit, with a 5-phase AC generator supplying a full-wave bridge rectifier to provide a 28 V DC power supply. The generator field is fed from the rectified output of a directly-coupled exciter, with a stationary field and a 3-phase rotating armature. The exciter field is supplied from the output of solid-state AVR, which monitors the DC output voltage of the generator, compares the result with a reference voltage to form an error signal, and uses this to provide the necessary adjustment of the exciter field voltage.

The paper uses a mathematical model [1,2] for the power unit shown in Fig. 1. This model is based on tensor methods to represent AC generator-fed bridge rectifier systems which are well established [3,4]. The paper extends this technique of analysis to study the transient performance of the system when the generator is subjected to sudden load application, reduction or even when it is connected to a dynamic load which may regenerate power into the system. The predicted results presented show an excellent agreement with those from experimental measurements.

2- MAIN GENERATOR AND EXCITER MODELS

The computer program which simulates both main generator and the exciter, uses tensor methods to generate automatically the mesh differential equations which correspond to the diode conduction patterns in both generator and exciter rectifier bridges. Since the method is well documented elsewhere [1,2,5] it is only outlined below.

The method requires branch and mesh reference frames to be defined for the generator unit, together with the transformations between them. Using happ's tensor notation [6], the equations involved are for the branch reference frame.

$$E_b + V_b = (R_b + G_b)I^b + L_b p\, I_b \tag{1}$$

For the mesh reference frame

$$E_m + V_m = (R_m + G_m)I^m + L_m p\, I_m \tag{2}$$

The necessary transformations are

$$I^b = C^{b}_{.m} I^m \tag{3}$$

$V_m = 0$ (Null vector : Kirchhoff's voltage law).

$$E_m = C^{.b}_{m} E_b \tag{4}$$

$$R_m = C^{.b}_{m} R_b C^{b}_{.m}$$

$$G_m = C^{.b}_{m} R_b G^{b}_{.m} \tag{5}$$

$$L_m = C^{.b}_{m} L_b C^{b}_{.m}$$

If eqns (4) and (5) are substituted in eqn (2) the result may be rearranged to give

$$pI^m = (C^{.b}_{m} L_b C^{b}_{.m})^{-1} \; C^{.b}_{m} E_b - C^{.b}_{m} (R_b + G_b)\, C^{b}_{.m} I^m \tag{6}$$

Eqn (6) may be integrated numerically to give step-by-step solution for the mesh current vector I^m . From this, the branch current vector I^b may be derived using eqn (3) and the branch voltage vector V_b using eqn. (1)

Some of the elements of the branch inductance matrix L_b and the branch rate-of-change of inductance matrix $[G_b]$ are time varying, according to the rotor positions of the main generator and the exciter, and these need to be updated accordingly at each step of the integration process. The elements of the transformation tensors $C^b_{.m}$ and $C^{.b}_{m}$ vary according to the conduction patterns of the two diode bridges, and these are updated automatically by the computer program.

3- AVR DESCRIPTION AND MODEL

The AVR model is developed from its actual circuit arrangements [1,2,5], instead of the usual transfer function representation which is subject to both simplification and linearisation. A complete circuit diagram for the AVR is given in Fig. 2, with the main functional blocks enclosed by dotted lines. The output voltage of the main generator is attenuated by resistors R_1, R_3 and R_{19} before being compared with the 6.2 V DC reference in the linear error amplifier IC1. A traingular voltage waveform is generated at the inverted terminal of the oscillator IC2, with a repetion rate set by R_{10} and C_7. The triangular waveform is compared with the output of IC1 in the comparator amplifier IC3 such that the output from this amplifier is either 0 or + 20 V depending on whether the instantaneous value of the triangular waveform is respectively greater than or less than the eror amplifier voltage. The resulting rectangular pulse train of voltage has the same repetition rate as the oscillator, but a Mark/Space ratio which decreases as the input voltage to the AVR increases. Transistors TR1 to TR3 switch according to the output of IC3 to provide a 28 V pulse train, which is applied to the exciter field. Again, the increase or decrease of the Mark/Space ratio, which depends respectively on the decrease or increase of the AVR input voltage, provides the control necessary to maintain constant the main generator terminal voltage.

To provide greater accuracy, modelling of the sensing and error amplifier circuit was achieved by developing the circuit equations which are arranged in the state-variable form using the capacitor voltage and the eror amplifier output voltage as the state variables.

4- LOAD APPLICATION AND REDUCTION

Sudden load application or reduction is provided experimently by using a change-over switch as shown in Fig. 3. Modelling of load application or reduction was achieved by respectively increasing or decreasing the value or load impedance.

4-1 Results

It is noticeable that the sudden drop in the generator output voltage, evident in fig. 5-a at the instant of load application, causes an almost immediate rise in the error amplifier voltage of Fig. 6-a. This in turn increases the width of the voltage pulses to the excited field, as seen in Fig. 6-b. It is further evident that the increased load current, Fig. 5-b, results in an increased ripple in the generator output voltage. It will be seen that the pulse width of Fig. 6-b decreases steadily toward its original value as the system approaches its steady state, and the generator output voltage moves back towards the regulated value.

Same remarks but in opposit way could be noticed when load is reduced. It is apparent that the effect of the sudden load reduction on the generator output voltage, evident in Fig. 7-a causes the output voltage of the error amplifier to experience the drop seen in Fig. 8-a. Considerations of the exciter field voltage of Fig. 8-b indicate that the power transistors in the AVR have cut off for some 20 ms, so as to force the generator ouptut voltage to drop to the regulated value.

5- DYNAMIC LOAD

The performance of the system model was investigated when it suplied the dynamic load presented in Fig. 4, which may regenerate power into the system. The output circuit comprises a battery and a capacitor, connected in parallel, with the dynamic load being represented by a DC voltage source in series with an impedance Z_L. The level of this voltage source may be increased to cause regeneration into the system.

5-1 Output Circuit Analysis

The generator output circuit of Fig. 4, may be represented mathematically by the equations :

$$\frac{dV_c}{dt} = \frac{1}{C}(I_{Gn} - I_B) \qquad (7)$$

$$V_c - (R_d + R_{bt})\, I_B - (PL_d + PL_{bt})\, I_B + (R_{bt} + PL_{bt})\, I_L - E_{bt} = 0 \qquad (8)$$

$$E_{bt} - (R_{bt} + R_L)\, I_L - (PL_{bt} + PL_L)\, I_L + (R_{bt} + PL_{bt})\, I_B - E_L = 0 \qquad (9)$$

which may be rearranged int he form

$$PV_c = \frac{1}{C} (I_{Gn} - I_B) \tag{10}$$

$$PI_L = \frac{1}{LS} (V_c L_{bt} - E_L L_u + E_{bt} L_x + Q_1 I_B + Q_2 I_L) \tag{11}$$

$$PI_B = \frac{1}{LS} (V_c L_v + E_{bt} L_y - E_L L_{bt} + Q_3 I_B + Q_4 I_L) \tag{12}$$

in which

$L_u = L_{tl} + L_{bt}$ $\quad$ $L_y = L_{bt} - L_v$

$L_v = L_L + L_{bt}$ $\quad$ $Q_1 = R_{bt} L_u - R_1 L_{bt}$

$R_1 = R_{tl} + R_{bt}$ $\quad$ $Q_1 = R_{bt} L_{bt} - R_2 L_u$

$R_2 = R_L + R_{bt}$ $\quad$ $Q_3 = R_{bt} L_{bt} - R_1 L_v$

$LS = L_u L_v - L_{bt}^2$ $\quad$ $Q_4 = R_{bt} L_v - R_2 L_{bt}$

$L_x = L_u - L_{bt}$

5-2 Computer Implementation

The computer program introduced above requires a modification to enable it to accommodate equations 10, 11, 12. In the numerical solution, these equations are integrated numerically to obtain the voltage across the capacitor V_c, the capacitor/battery mesh current I_B, and the load/battery mesh current I_L. The battery branch current then follows from

$$I_{bt} = I_B - I_L$$

and the battery branch voltage from

$$V_{bt} = E_{bt} + R_{bt} I_{bt} + L_{bt} \left(\frac{dI_B}{dt} - \frac{DI_L}{dt}\right)$$

ouptut circuit parameters

The parameters of the output circuit are specified in Fig. 4. The battery voltage is set at 26.65 V. The voltage source representing the load is set initially at 11.5 V, for which the current into the load is 300 A. This voltage is then increased suddenly to 38.5 V, which in the final steady-state forces a current of 150 A back into thė system.

5-3 Predicted Results

The waveforms presented in Fig 9 indicate the system performance for the generator when connected to dynamic load. The ripple evident in the load current waveform of fig. 9-i is due to the bridge rectifier, and it will be noted that this ripple disappears when the rectifier cuts-off and current is no longer supplied to the load circuit from the generator. Consideration of the capacitor voltage shows a noticable jump at the instant of load switching, together with a ripple which decreases as the forward load current decreases. After the rectifier has cut-off, the capacitor voltage reaches a DC level determined by the battery voltage E_{bt}, the voltage source E_L and the output circuit parameters. The jump in the capacitor voltage causes the error amplifier voltage of Fig. 9-m to fall, and eventually to cut-off the exciter field voltage as shown in Fig. 9-n. The DC component in the exciter field current of Fig. 9-p decreases after load switching, with a reduction occuring also in the exciter line and phase currents of Figs. 9-j and 9-k and in the exciter phase voltage of Fig. 9-l. The generator line and phase currents of of Figs. 9-a and 9-b gradually decreases after load switching, until the rectifier eventually cuts-off. The following effects are evident when the rectifier cuts-off :

(a) The distortion in the generator phase voltage of Fig. 9-c disapears;
(b) The harmonic content in the generator field current of Fig. 9-d also disapears;
(c) The frequency modulation in the generator field voltage of Fig. 9-e is no longer present, and
(d) The ripple in the capacitor voltge waveform of Fig. 9-h disappears.

The battery branch current and voltage of Fig. 9-f and 9-g both show a jump when the load is switched, and they eventually contain only a DC component as the system reaches its steady-state.

6- CONCLUSIONS

The close agreement between experimental and predicted waveforms has provided further validation of the bruchless DC generator model and it may now be used with confedence, both as a tool for improving generator performance and as a component in larger system studies.

The case of regeneration is particularly interesting, since the AVR then loses control of the output voltage as the rectifier cuts off, and the generator voltage has no effect on the output voltage. This situation is of course not valid for a conventional DC generator, which is capable of regeneration and is never disconnected from the system.

REFERENCES

1- Gerges, W.R., Kettleborough J.G. and Smith, I.R. "Mathematical modelling of a brushless DC generator", IASTED International Symposium on Simulation, Modelling and Development - SMD'87, Cairo, March 3-5, 1987.

2- Vadher, V.V., Kettleborough, J.G., Smith, I.R. and Gerges, W.R. "Generalised Model of Brushless DC Generator", IEEE Trans., Aerospace and Electronic Systems, Vol. 25 No. 4, July, 1989.

3- Kettleborough, J.G., Smith, I.R. and Fanthome, B.A. "Simulation of dedicated aircraft generator supplying a heavy rectified load", Proc. IEE, Vol 130, Pt B, No. 6, Nov. 1983.

4- Gregory, K., Kettleborough, J.G., Fanthome, B.A., Fitton, C.R and Smith, I.R., "Simulation of parallel connected brushless DC generators' IASTED Third Int. Symposium on Modelling, Identification and Control, Innsbruck, pp. 5-9, Feb. 1984.

5- Gerges, W.R., "Mathematical model of an AVR controlled brushless 5-phase generator", Ph.D. Thesis, Loughborough University of Technology, Nov. 1985.

6- Happ, H.H., "Diakoptics and Networks", (Academic Press, 1971).

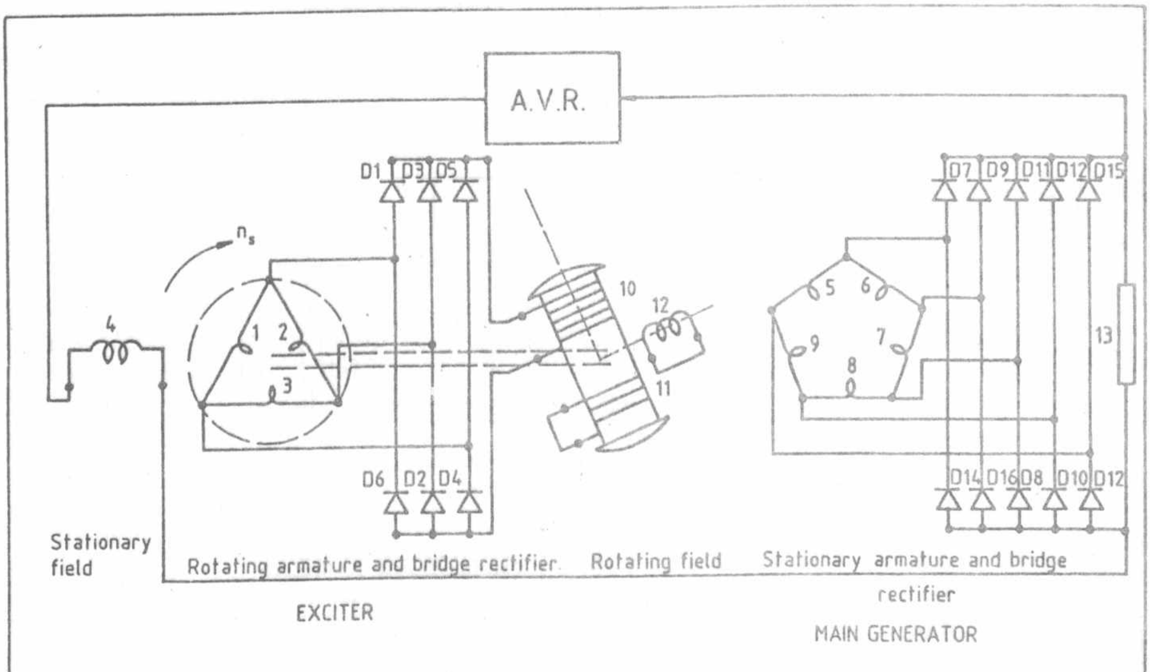

FIG. 1 COMPLETE POWER SYSTEM

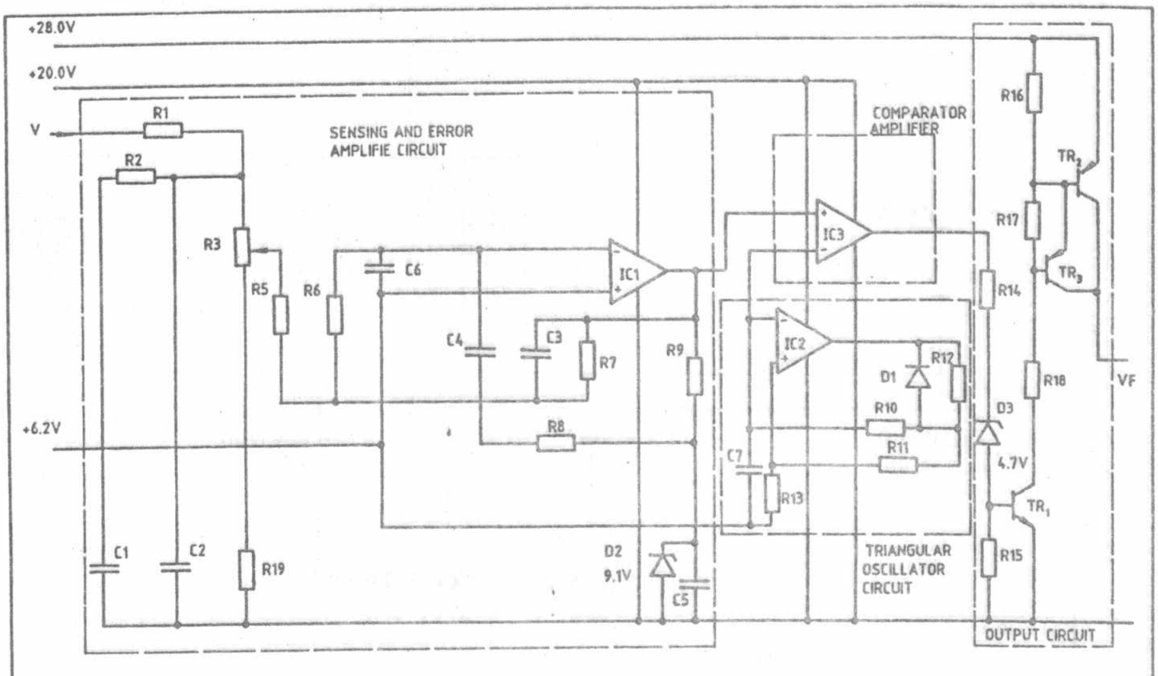

FIG. 2 A.V.R. CIRCUIT DIAGRAM

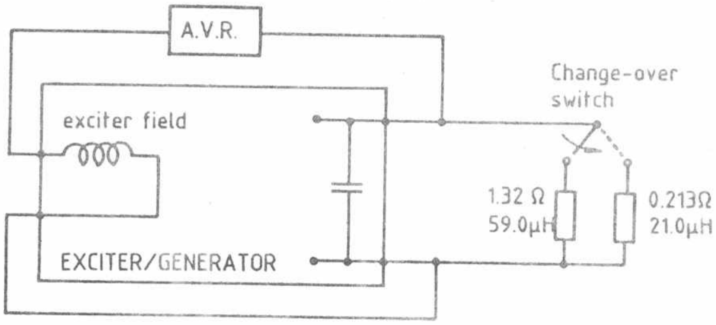

FIG 3 CIRCUITS FOR LOAD APPLICATION AND REJECTION

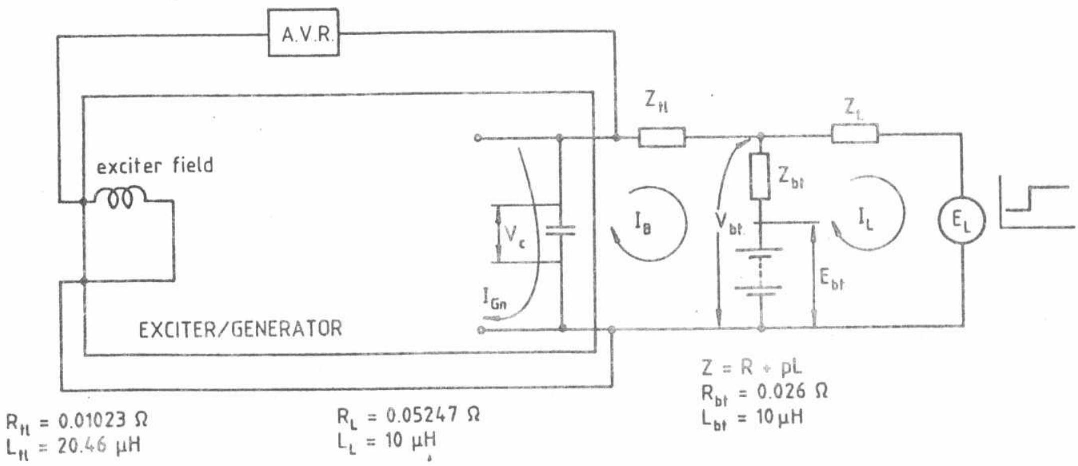

FIG 4 CIRCUIT USED TO SIMULATE DYNAMIC LOAD

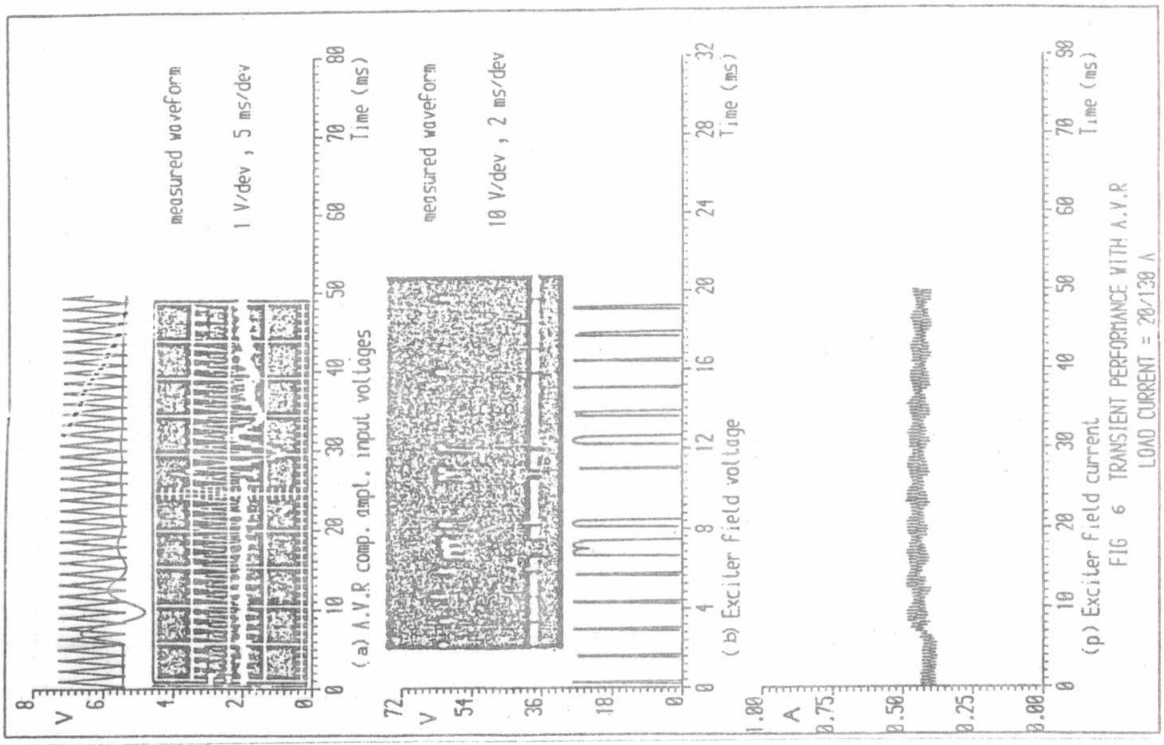

FIG 6 TRANSIENT PERFORMANCE WITH A.V.R
LOAD CURRENT = 20/130 A

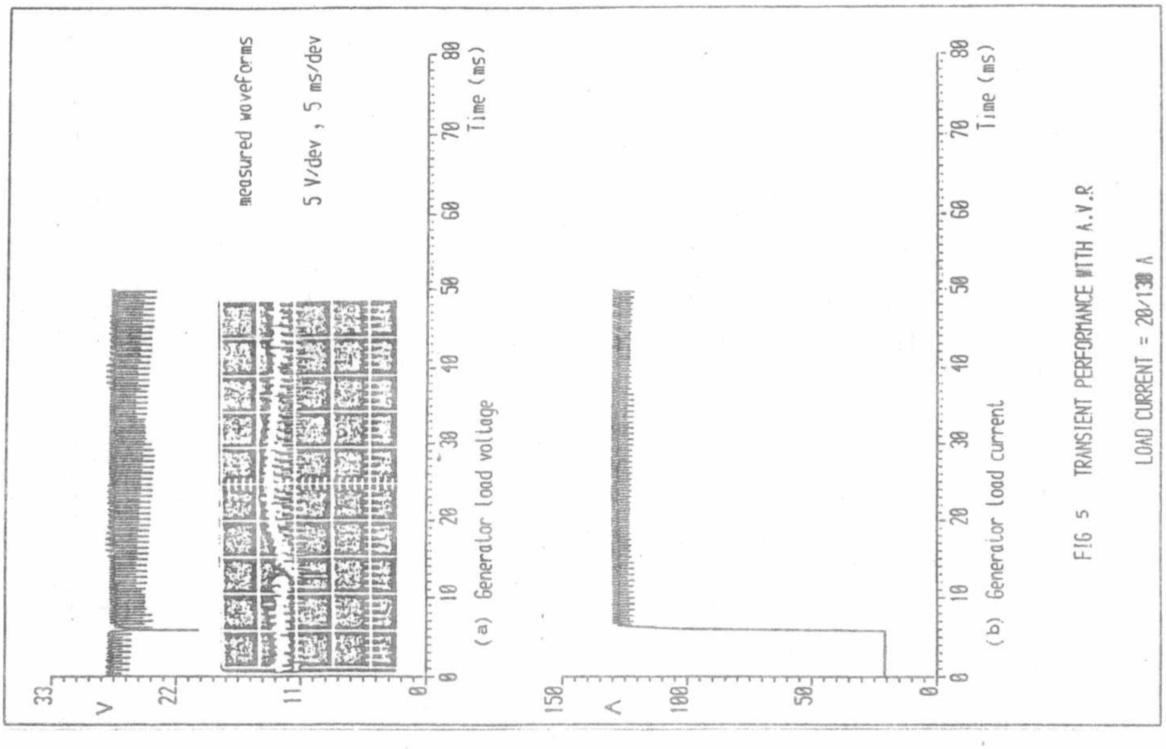

FIG 5 TRANSIENT PERFORMANCE WITH A.V.R

LOAD CURRENT = 20/130 A

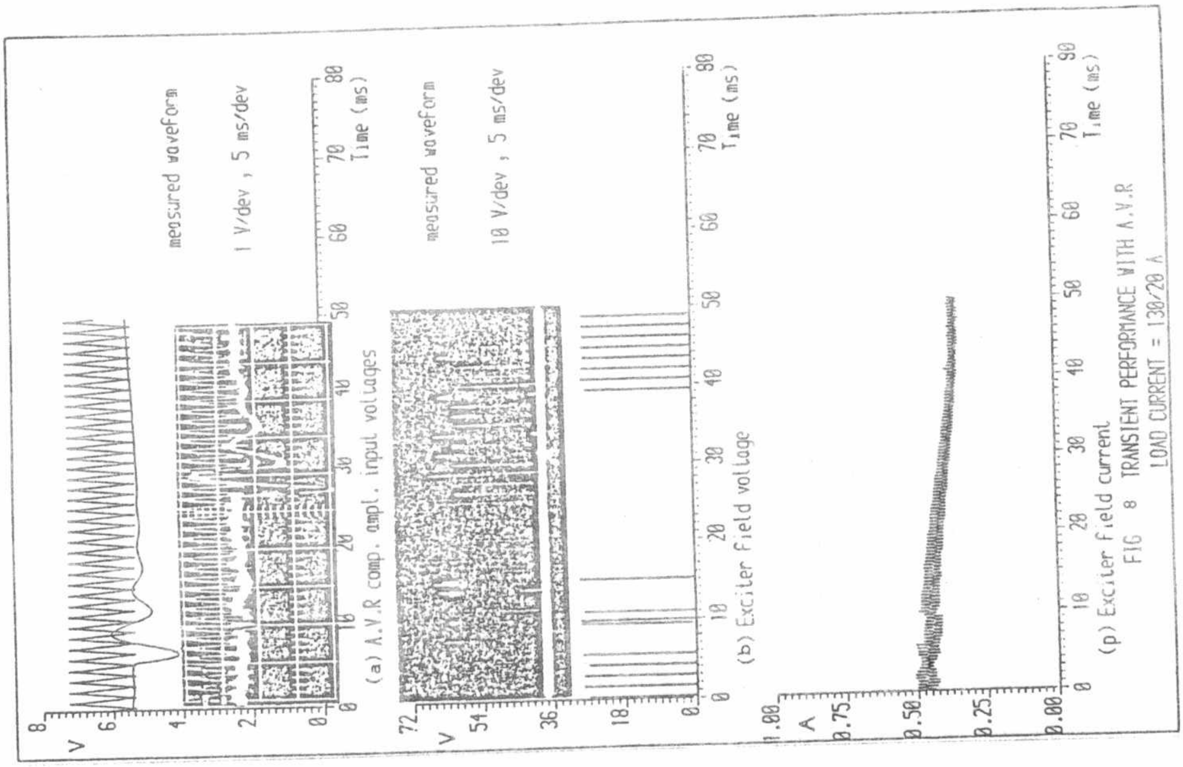

FIG 8 TRANSIENT PERFORMANCE WITH A.V.R
LOAD CURRENT = 130/20 A

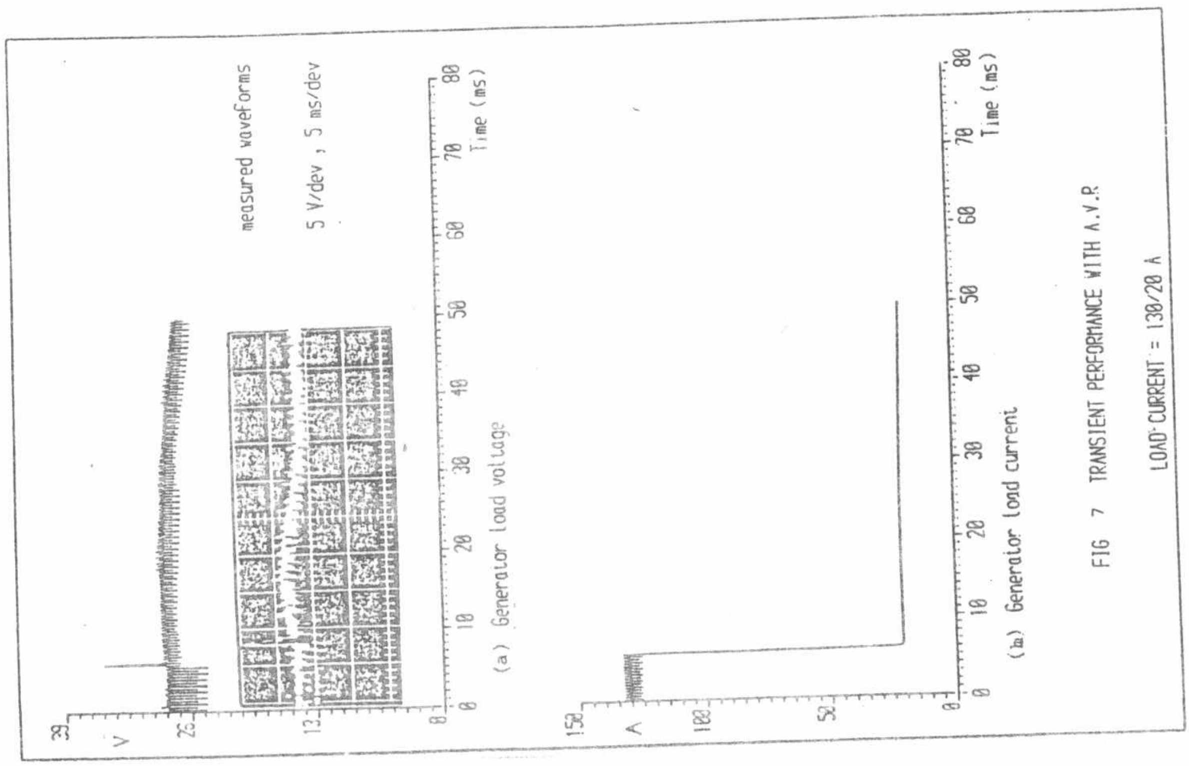

FIG 7 TRANSIENT PERFORMANCE WITH A.V.R
LOAD CURRENT = 130/20 A

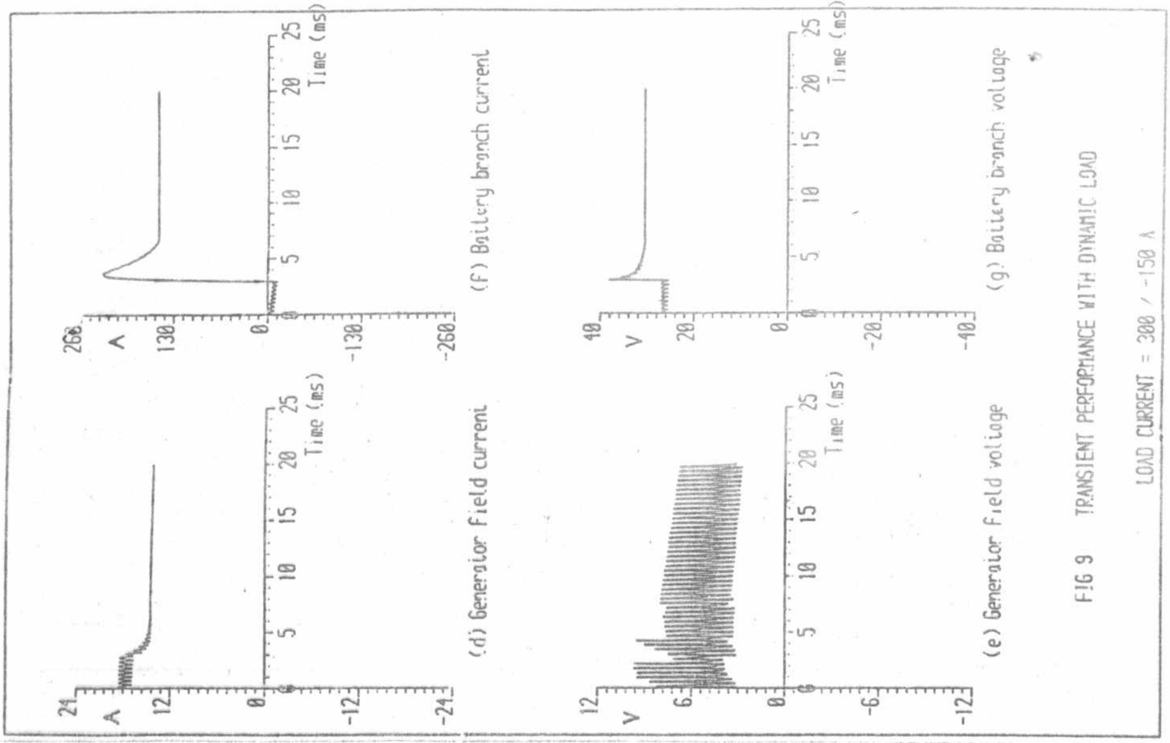

FIG 9 TRANSIENT PERFORMANCE WITH DYNAMIC LOAD

LOAD CURRENT = 300 / -150 A

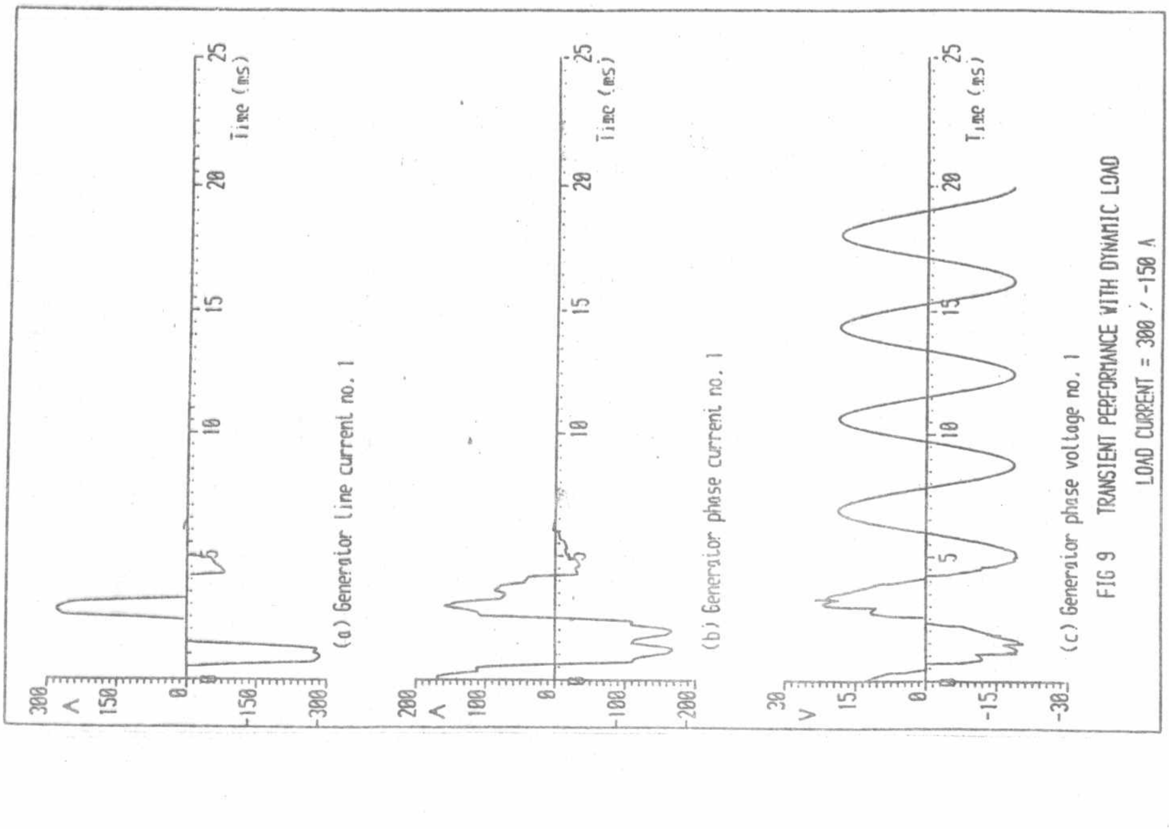

FIG 9 TRANSIENT PERFORMANCE WITH DYNAMIC LOAD

LOAD CURRENT = 300 / -150 A

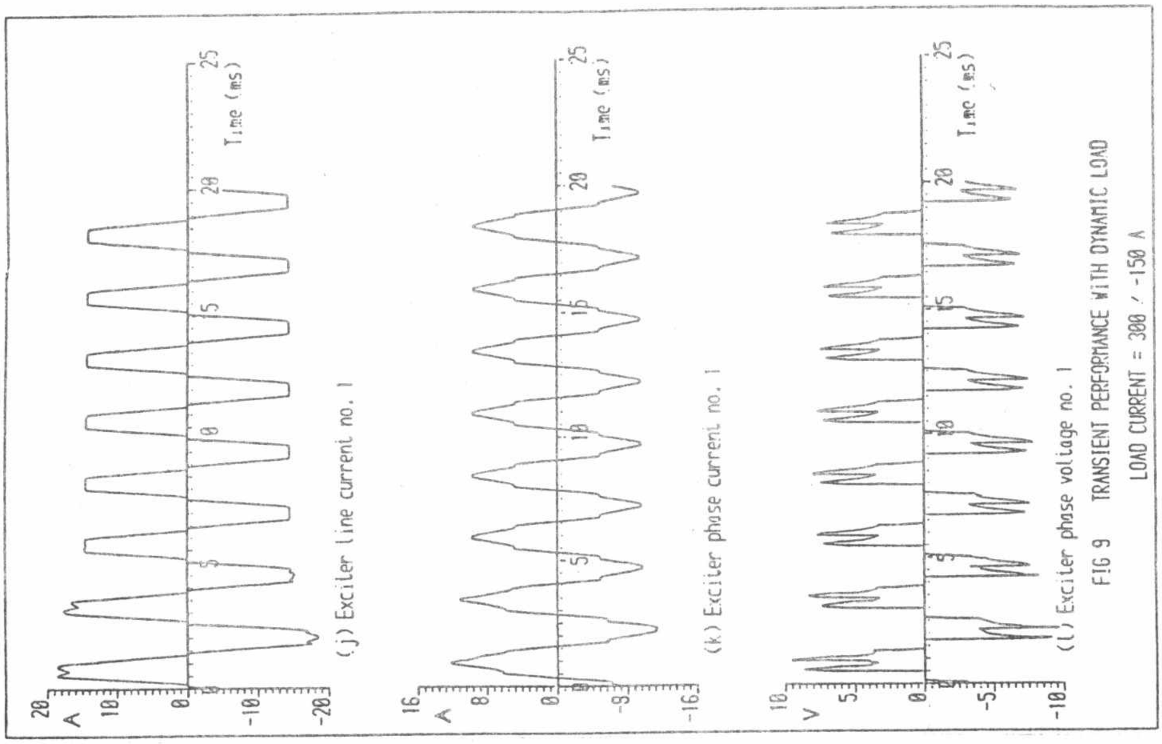

FIG 9 TRANSIENT PERFORMANCE WITH DYNAMIC LOAD

LOAD CURRENT = 300 / -150 A

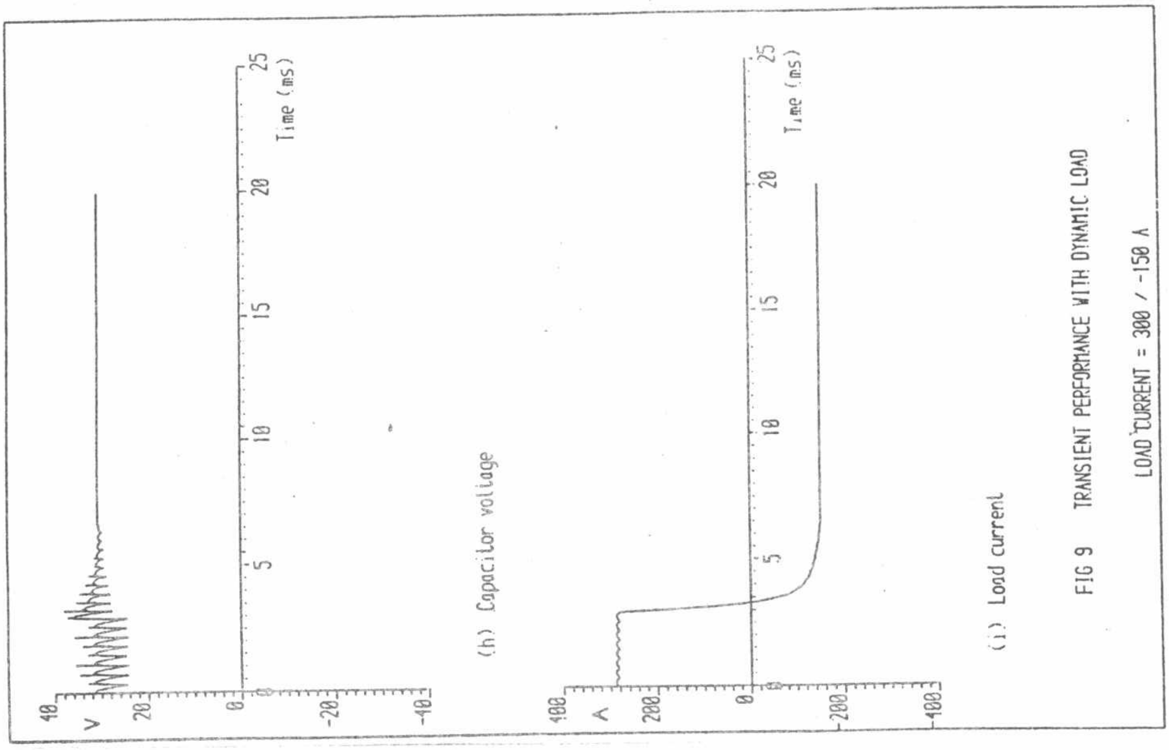

FIG 9 TRANSIENT PERFORMANCE WITH DYNAMIC LOAD

LOAD CURRENT = 300 / -150 A

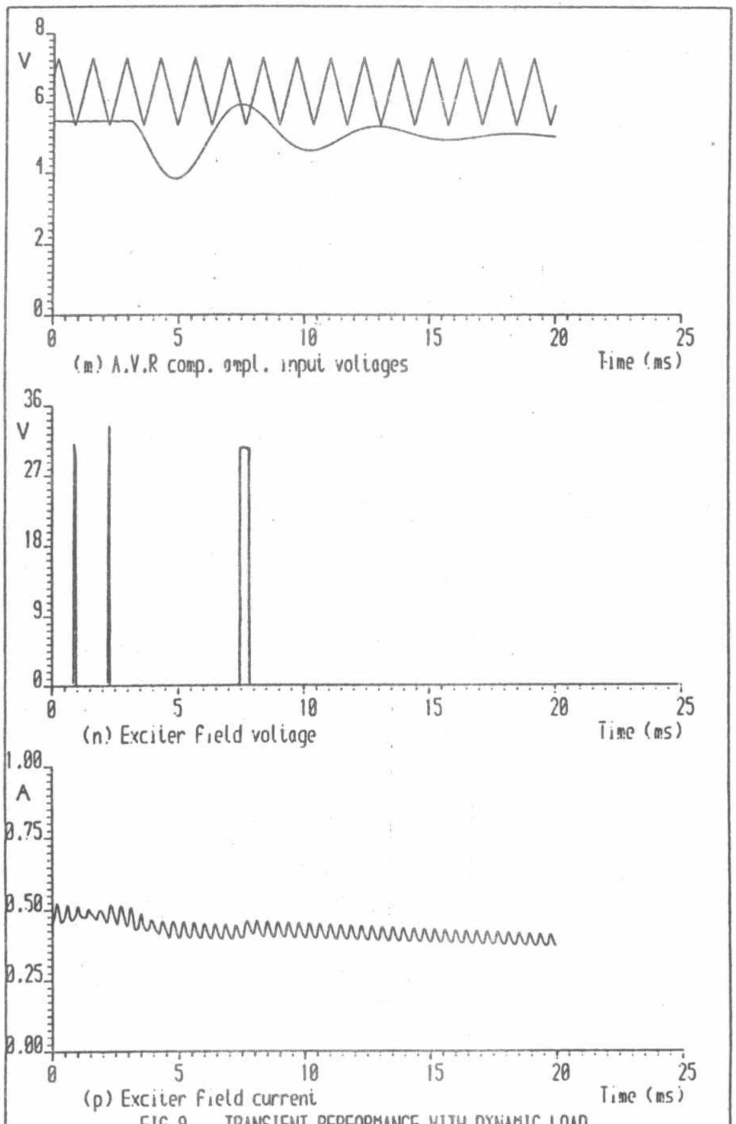

FIG 9 TRANSIENT PERFORMANCE WITH DYNAMIC LOAD
LOAD CURRENT = 300 / -150 A